Aqua, Alcohol, and Acetonitrile Adducts of Tris(perfluorophenyl)borane: Evaluation of Brønsted Acidity and Ligand Lability with Experimental and Computational Methods

Catherine Bergquist, Brian M. Bridgewater, C. Jeff Harlan, Jack R. Norton,* Richard A. Friesner,* and Gerard Parkin*

Contribution from the Department of Chemistry, Columbia University, New York, New York 10027

Received May 31, 2000

Abstract: Equilibrium studies have been performed to determine the Brønsted acidity of $[(C_6F_5)_3B(OH_2)]\cdot H_2O$, the aqua species that exists in acetonitrile solutions of $B(C_6F_5)_3$ in the presence of water. NMR spectroscopic analysis of the deprotonation of $[(C_6F_5)_3B(OH_2)]\cdot H_2O$ with 2,6-$Bu^t_2C_5H_3N$ in acetonitrile allows a pK value of 8.6 to be determined for the equilibrium $[(C_6F_5)_3B(OH_2)]\cdot H_2O \rightleftarrows [(C_6F_5)_3B(OH)]^- + [H_3O]^+$. On the basis of a calculated value for the hydrogen bond interaction in $[(C_6F_5)_3B(OH_2)]\cdot H_2O$, the p$K_a$ for $(C_6F_5)_3B(OH_2)$ is estimated to be 8.4 in acetonitrile. Such a value indicates that $(C_6F_5)_3B(OH_2)$ must be regarded as a strong acid, with a strength comparable to that of HCl in acetonitrile. Dynamic NMR spectroscopic studies indicate that the aqua and acetonitrile ligands in $(C_6F_5)_3B(OH_2)$ and $(C_6F_5)_3B(NCMe)$ are labile, with dissociation of H_2O being substantially more facile than that of MeCN, by a factor of ca. 200 in rate constant at 300 K. Ab initio calculations were performed in the gas phase and with a dielectric solvent model to determine the strength of B−L bonds (L = H_2O, ROH, MeCN) and hydrogen bonds involving B−OH_2 and B−O(H)R derivatives.

Introduction

Tris(perfluorophenyl)borane, $B(C_6F_5)_3$,[1] is a potent Lewis acid that has recently found extensive use as an activator for metallocene polymerization catalysts of the type $(Cp^R)_2MMe_2$.[2] Correspondingly, the aqua complexes, $(C_6F_5)_3B(OH_2)$[3] and $[(C_6F_5)_3B(OH_2)]\cdot 2H_2O$, as illustrated in Figure 1, are known to behave as Brønsted acids.[4,5] For example, we have recently used $(C_6F_5)_3B(OH_2)$ to protonate the tris(3-*tert*-butyl-5-methyl)-pyrazolylhydroborato zinc hydroxide complex $[Tp^{Bu^t,Me}]ZnOH$ and give the aqua species $\{[Tp^{Bu^t,Me}]Zn(OH_2)]\}[HOB(C_6F_5)_3]$.[6] In this paper, we describe quantitative aspects of the solution chemistry of aqua derivatives of $B(C_6F_5)_3$, including determination of the Brønsted acidity of $[(C_6F_5)_3B(OH_2)]\cdot H_2O$ in acetonitrile.

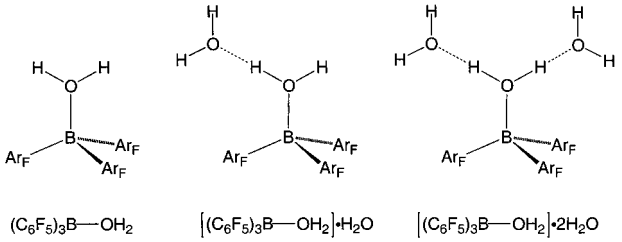

Figure 1. Aqua derivatives of $B(C_6F_5)_3$: $(C_6F_5)_3B(OH_2)$, $[(C_6F_5)_3B(OH_2)]\cdot H_2O$, and $[(C_6F_5)_3B(OH_2)]\cdot 2H_2O$.

Results and Discussion

(i) Brønsted acidity of $[(C_6F_5)_3B(OH_2)]\cdot H_2O$. Previous studies have reported that the Lewis acidity of $B(C_6F_5)_3$ is comparable to that of BF_3; thus, with the Lewis acidity of BBr_3 taken as unity, that of BF_3 is 0.77, while that of $B(C_6F_5)_3$ has a value of 0.72.[7−9] However, despite the fact that aqua derivatives of $B(C_6F_5)_3$ have also been employed as Brønsted acids in nonaqueous solvents, their Brønsted acidity has not been quantified. It is, therefore, pertinent to establish the Brønsted acidity of such aqua species in a nonaqueous solvent.

A meaningful quantification of the Brønsted acidity mandates that the *solution* nature of the aqua species present in the organic

(1) For a review of the applications of $B(C_6F_5)_3$, see: Piers, W. E.; Chivers, T. *Chem. Soc. Rev.* **1997**, *26*, 345−354.

(2) For the first literature report of $B(C_6F_5)_3$ as a metallocene activator, see: Yang, X.; Stern, C. L.; Marks, T. J. *J. Am. Chem. Soc.* **1991**, *113*, 3623−3625.

(3) For the first reports of $(C_6F_5)_3B(OH_2)$, see: (a) Siedle, A. R.; Lamanna, W. M. U.S. Patent No. 5,296,433, March 22, 1994. (b) Bradley, D. C.; Harding, I. S.; Keefe, A. D.; Motevalli, M.; Zheng, D. H. *J. Chem. Soc., Dalton Trans.* **1996**, 3931−3936.

(4) See, for example: (a) Siedle, A. R.; Lamanna, W. M.; Newmark, R. A.; Stevens, J.; Richardson, D. E.; Ryan, M. *Makromol. Chem. Macromol. Symp.* **1993**, *66*, 215−224. (b) Danopoulos, A. A.; Galsworthy, J. R.; Green, M. L. H.; Cafferkey, S.; Doerrer, L. H.; Hursthouse, M. B. *Chem. Commun.* **1998**, 2529−2530. (c) Doerrer, L. H.; Green, M. L. H. *J. Chem. Soc., Dalton Trans.* **1999**, 4325−4329.

(5) Furthermore, in situ generated $(C_6F_5)_3B(OH_2)$ has also been used as a proton acid. See, for example: (a) Hill, G. S.; Manojlovic-Muir, L.; Muir, K. W.; Puddephatt, R. J. *Organometallics* **1997**, *16*, 525−530. (b) Shaffer, T. D.; Ashbaugh, J. R. *J. Polym. Sci: Part A: Polym. Chem.* **1997**, *35*, 329−344.

(6) Bergquist, C.; Parkin, G. *J. Am. Chem. Soc.* **1999**, *121*, 6322−6323.

(7) Döring, S.; Erker, G.; Fröhlich, R.; Meyer, O.; Bergander, K. *Organometallics* **1998**, *17*, 2183−2187.

(8) Jacobsen, H.; Berke, H.; Döring, S.; Kehr, G.; Erker, G.; Fröhlich, R.; Meyer, O. *Organometallics* **1999**, *18*, 1724−1735.

(9) The Lewis acidity scale is based on the magnitude of the change of ^1H and ^{13}C NMR spectroscopic shifts of α,β-unsaturated carbonyl and nitrile compounds upon complexation to a Lewis acid. See: (a) Childs, R. F.; Mulholland, D. L.; Nixon, A. *Can. J. Chem.* **1982**, *60*, 801−808. (b) Childs, R. F.; Mulholland, D. L.; Nixon, A. *Can. J. Chem.* **1982**, *60*, 809−812. (c) Laszlo, P.; Teston, M. *J. Am. Chem. Soc.* **1990**, *112*, 8750−8754.

10.1021/ja001915g CCC: $19.00
Published on Web 10/18/2000

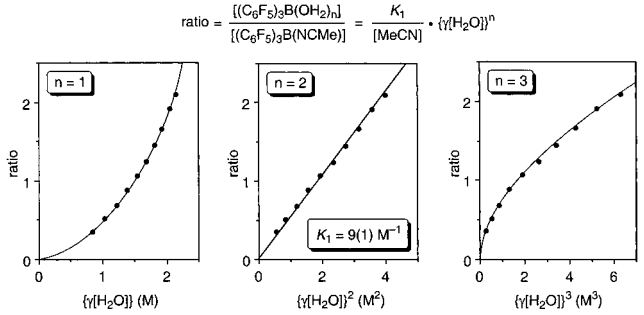

Figure 2. Plots of the ratio $[(C_6F_5)_3B(OH_2)_n]/[(C_6F_5)_3B(NCMe)]$ versus $\{\gamma[H_2O]\}^n$ for $n = 1$, 2, and 3 (γ = activity coefficient). The experiment was carried out twice and the value of K_1 is the average of two determinations.

medium be first determined. That such a study is necessary is highlighted by the fact that several different aqua complexes have been structurally characterized in the solid state, including $(C_6F_5)_3B(OH_2)$[4c,10] and $[(C_6F_5)_3B(OH_2)]\cdot 2H_2O$.[4b] The latter complex reacts readily with $B(C_6F_5)_3$ to generate $(C_6F_5)_3B(OH_2)$,[4a] thereby suggesting that the thermodynamic preference for one species over another is not strong.

Acetonitrile was selected as the solvent of choice for these studies due to the wealth of available pK_a information.[11,12] In the absence of water, $B(C_6F_5)_3$ reacts immediately with acetonitrile to give the four-coordinate adduct $(C_6F_5)_3B(NCMe)$.[8,13] The adduct formation is, however, sufficiently weak that the acetonitrile may be displaced by water, and equilibrium titration studies (see Supporting Information for spectra) demonstrate that the reaction of $(C_6F_5)_3B(NCMe)$ with H_2O is characterized by eq 1. The equilibrium may be conveniently studied by ^{19}F NMR spectroscopy, since the reaction is sufficiently slow that both $(C_6F_5)_3B(OH_2)_n$ and $(C_6F_5)_3B(NCMe)$ may be observed.

$$(C_6F_5)_3B{-}NCMe + 2H_2O \overset{K_1}{\rightleftharpoons} \left|(C_6F_5)_3B{-}OH_2\right|\cdot H_2O + MeCN \quad (1)$$

Evidence for the stoichiometry of the reaction between $(C_6F_5)_3B(NCMe)$ and H_2O is provided by measurement of the variation of the ratio of $[(C_6F_5)_3B(OH_2)_n]$:$[(C_6F_5)_3B(NCMe)]$ as a function of $\{\gamma[H_2O]\}^n$, where γ is the activity coefficient;[14] only for a value of $n = 2$ is a good linear dependence observed in a plot of $\{[(C_6F_5)_3B(OH_2)_n]/[(C_6F_5)_3B(NCMe)]\}$ vs $\{\gamma[H_2O]\}^n$ (Figure 2). The ratio of $[(C_6F_5)_3B(OH_2)_n]$:$[(C_6F_5)_3B(NCMe)]$ in a given sample is strongly temperature dependent, as illustrated by Figure 3, from which ΔH_1 and ΔS_1 may be estimated to be $-8.6(5)$ kcal mol^{-1} and $-25(2)$ eu.[15]

Interestingly, the composition of the aqua species present in acetonitrile solution, $[(C_6F_5)_3B(OH_2)]\cdot H_2O$, is intermediate between those of the two aqua complexes that have been

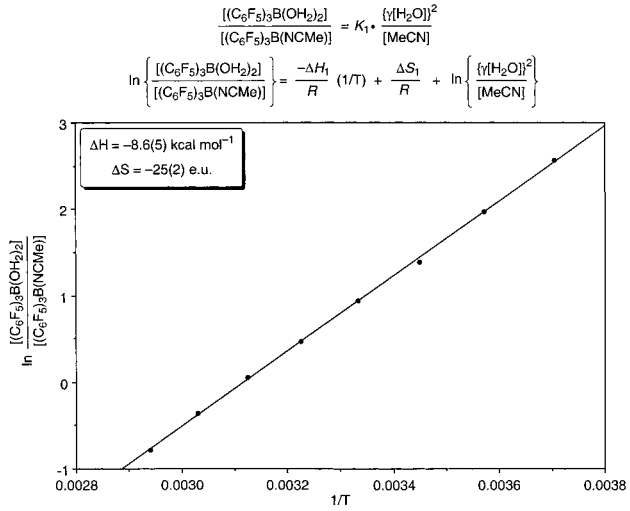

Figure 3. Temperature dependence of the ratio $[(C_6F_5)_3B(OH_2)_2]/[(C_6F_5)_3B(NCMe)]$.

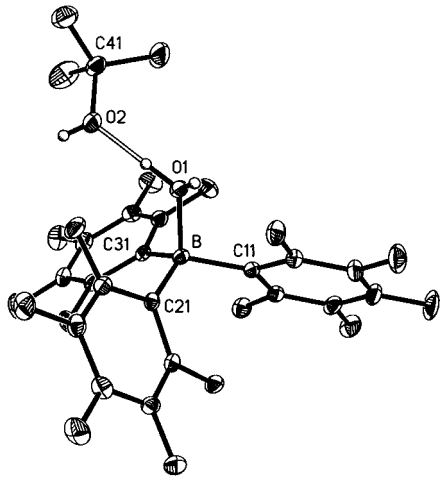

Figure 4. Molecular structure of $[(C_6F_5)_3B(OH_2)]\cdot HOBu^t$. Selected bond lengths (Å) and angles (deg): B−O(1) 1.583(3), B−C(11) 1.629(4), B−C(21) 1.621(4), B−C(31) 1.639(4), O(1)···O(2) 2.510(4); O(1)−B−C(11) 103.9(2), O(1)−B−C(21) 108.5(2), O(1)−B−C(31) 102.9(2), C(11)−B−C(21) 110.9(2), C(11)−B−C(31) 115.4(2), C(21)−B−C(31) 114.2(2), B−O(1)···O(2) 121.1(1).

structurally characterized in the solid state, namely $(C_6F_5)_3B(OH_2)$ and $[(C_6F_5)_3B(OH_2)]\cdot 2H_2O$.[4b,c,10,16] By analogy with $[(C_6F_5)_3B(OH_2)]\cdot 2H_2O$, the structure of $[(C_6F_5)_3B(OH_2)]\cdot H_2O$ is proposed to have a single hydrogen bond interaction with the coordinated water molecule (Figure 1). Support for this suggestion is provided by the structural characterization of the analogous alcohol complexes $[(C_6F_5)_3B(OH_2)]\cdot HOBu^t$ (Figure 4) and $[(C_6F_5)_3B(HOMe)]\cdot HOMe$ (Figure 5), which are obtained by the reactions of $B(C_6F_5)_3$ with Bu^tOH/H_2O and MeOH, respectively (Scheme 1).[17]

(10) A species of composition $[(C_6F_5)_3B(OH_2)]\cdot$dioxane$\cdot CH_2Cl_2$ has also been structurally characterized by X-ray diffraction. See: Janiak, C.; Braun, L.; Scharmann, T. G.; Girgsdies, F. *Acta Crystallogr.* **1998**, *C54*, 1722−1724.

(11) Izutsu, K. *Acid−Base Dissociation Constants in Dipolar Aprotic Solvents*; Blackwell Scientific Publications: Boston 1990.

(12) See, for example: (a) Kristjánsdóttir, S. S.; Norton, J. R. In *Transition Metal Hydrides*; Dedieu, A., Ed.; VCH: New York, 1992; Chapter 9, pp 309−359. (b) Kristjánsdóttir, S. S.; Loendorf, A. J.; Norton, J. R. *Inorg. Chem.* **1991**, *30*, 4470−4471. (c) Moore, E. J.; Sullivan, J. M.; Norton, J. R. *J. Am. Chem. Soc.* **1986**, *108*, 2257−2263.

(13) ^{19}F NMR spectroscopic studies provide no evidence for $B(C_6F_5)_3$ in a solution of $(C_6F_5)_3B(NCMe)$ in toluene-d_8 (≈30 mM) in the presence of ca. 1 equiv of MeCN at 245 K. The equilibrium, therefore, lies strongly in favor of the acetonitrile adduct, as supported by the computational study.

(14) Since the activity coefficient of water in acetonitrile is strongly dependent on its concentration, the equilibrium expression for eq 1 incorporates water activity rather than its concentration (see Experimental Section).

(15) The temperature dependence of the ratio $[(C_6F_5)_3B(OH_2)_2]/[(C_6F_5)_3B(NCMe)]$ was measured for a sample of $(C_6F_5)_3B(OH_2)$ in CD_3CN in the presence of a large excess of water. Under these conditions, the activity of water, and thus the ratio $[MeCN]/\{\gamma[H_2O]\}^2$, remains effectively constant as the equilibrium adjusts. Assuming that γ does not vary significantly over this temperature range, the temperature dependence of the ratio $[(C_6F_5)_3B(OH_2)_2]/[(C_6F_5)_3B(NCMe)]$ reflects that of the equilibrium constant. The linearity of Figure 3 suggests that this is a valid approximation. While the slope of Figure 3 ($-\Delta H_1/R$) gives ΔH_1 directly, the intercept corresponds to $(\Delta S_1/R + \ln\{\{\gamma[H_2O]\}^2/[MeCN]\})$. The standard state is 1 M.

(16) $Ph_3B(OH_2)$ has also been structurally characterized as a cocrystallized species, $[(cyclam)Re(O)_2]Cl\cdot 2Ph_3B(OH_2)$. See: Blake, A. J.; Greig, J. A.; Schröder, M. *J. Chem. Soc., Dalton Trans.* **1988**, 2645−2647.

(17) $[(C_6F_5)_3B(HOMe)]\cdot HOMe$ was first described in ref 3a.

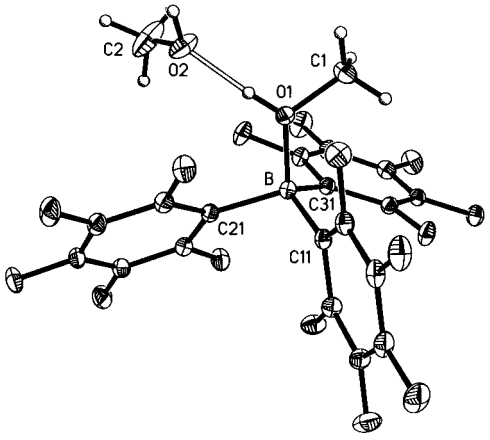

Figure 5. Molecular structure of $[(C_6F_5)_3B(HOMe)]\cdot HOMe$. Selected bond lengths (Å) and angles (deg): B−O(1) 1.557(2), B−C(11) 1.637(2), B−C(21) 1.639(2), B−C(31) 1.641(2), O(1)−C(1) 1.459(2), O(2)−C(2) 1.386(3), O(1)···O(2) 2.511(2); O(1)−B−C(11) 109.8(1), O(1)−B−C(21) 104.7(1), O(1)−B−C(31) 105.1(1), C(11)−B−C(21) 105.6(1), C(11)−B−C(31) 114.3(2), C(21)−B−C(31) 116.8(1), B−O(1)−C(1) 120.9(1), B−O(1)···O(2) 120.3(1).

Scheme 1

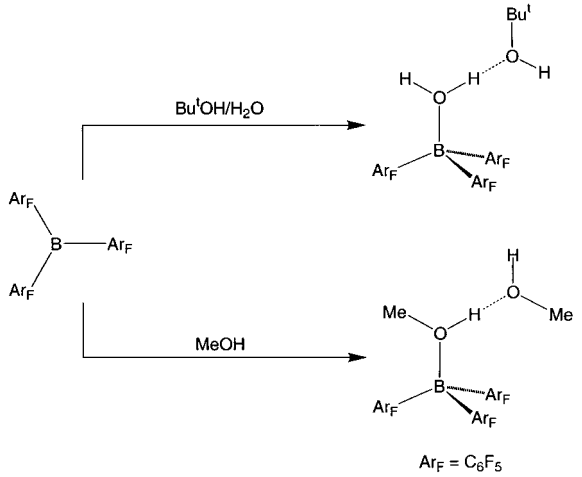

The Brønsted acidity of $[(C_6F_5)_3B(OH_2)]\cdot H_2O$ has been determined by titration with 2,6-di-*tert*-butylpyridine, 2,6-$Bu^t_2C_5H_3N$,[18] a suitable base for this purpose since its bulky *tert*-butyl substituents should minimize coordination to $B(C_6F_5)_3$.[19] Addition of 2,6-$Bu^t_2C_5H_3N$ to a solution of $[(C_6F_5)_3B(OH_2)]\cdot H_2O$ in acetonitrile results in proton transfer and the formation of $[2,6\text{-}Bu^t_2C_5H_3NH]^+$ and $[(C_6F_5)_3B(OH)]^-$, as demonstrated by NMR spectroscopy. The identity of the cation and anion were confirmed by independent experiments. For example, the cation $[2,6\text{-}Bu^t_2C_5H_3NH]^+$ was readily identified by ^{1}H NMR spectroscopic comparison with the species obtained by reaction of 2,6-$Bu^t_2C_5H_3N$ with triflic acid. Although $[(C_6F_5)_3B(OH)]^-$ derivatives are also known,[20] the ^{19}F NMR spectroscopic signals for $[(C_6F_5)_3B(OH)]^-$ are dynamically averaged with those of $[(C_6F_5)_3B(OH_2)]\cdot H_2O$,[21] thereby preventing definitive identification. However, an independent experiment involving addition of an excess of 1,8-bis(dimethylamino)naphthalene, "proton sponge", to $[(C_6F_5)_3B(OH_2)]\cdot H_2O$ in the presence of 3,5-bis(trifluoromethyl)bromobenzene, as both a ^{1}H and a ^{19}F NMR spectroscopic integration standard, has confirmed that the product has a stoichiometry of $[C_{10}H_6(NMe_2)_2H][(C_6F_5)_3B(OH)]$ and not, for example, $[C_{10}H_6(NMe_2)_2H][(C_6F_5)_3B(\mu\text{-}OH)B(C_6F_5)_3]$;[22] this suggests that MeCN (as a solvent), is a better Lewis base toward $B(C_6F_5)_3$ than is $[(C_6F_5)_3B(OH)]^-$. Thus, the concentration ratios of the various species present during the course of the titration of $[(C_6F_5)_3B(OH_2)]\cdot H_2O$ with 2,6-$Bu^t_2C_5H_3N$ may be extracted from the NMR spectroscopic data, thereby enabling the equilibrium constant for eq 2 (Scheme 2) to be determined (see Experimental Section).

Scheme 2

$$\left|(C_6F_5)_3B{-}OH_2\right|\cdot H_2O + 2,6\text{-}Bu^t_2C_5H_3N \overset{K_2}{\rightleftharpoons} \left|(C_6F_5)_3B{-}OH\right|^- + \left|2,6\text{-}Bu^t_2C_5H_3NH\right|^+ + H_2O \quad (2)$$

$$\left|2,6\text{-}Bu^t_2C_5H_3NH\right|^+ \overset{K_3}{\rightleftharpoons} 2,6\text{-}Bu^t_2C_5H_3N + H^+ \quad (3)$$

$$H_2O + H^+ \overset{K_4}{\rightleftharpoons} \left|H_3O\right|^+ \quad (4)$$

$$\left|(C_6F_5)_3B{-}OH_2\right|\cdot H_2O \overset{K_5}{\rightleftharpoons} \left|(C_6F_5)_3B{-}OH\right|^- + \left|H_3O\right|^+ \quad (5)$$

$$K_5 = K_2K_3K_4$$

Knowledge of the pK_a values for $[2,6\text{-}Bu^t_2C_5H_3NH]^+$ (11.4)[18] and H_3O^+ (2.2)[23] in acetonitrile (eqs 3 and 4) allows determination of the equilibrium constant for deprotonation of $[(C_6F_5)_3B(OH_2)]\cdot H_2O$ (eq 5) via the expression $K_5 = K_2K_3K_4$ (Table 1 and Scheme 2). Thus, K_5 may be determined to be 2.5×10^{-9} M, with a corresponding pK_5 value of 8.6.

It is important to emphasize that the deprotonation equilibrium described by eq 5 does not strictly correspond to a conventional K_a value in acetonitrile since $[(C_6F_5)_3B(OH_2)]\cdot H_2O$ and $[(C_6F_5)_3B(OH)]^-$ are not a true conjugate acid/base pair. Additionally, a K_a value in acetonitrile requires the proton to be solvated by MeCN and not H_2O, as is the case here. The observed equilibrium constant is, nevertheless, related to the more conventional K_a of $(C_6F_5)_3B(OH_2)$ via the thermodynamic cycle summarized in Scheme 3. Thus, $K_a = K_2K_3/K_6$, from which an estimate of the pK_a of $(C_6F_5)_3B(OH_2)$ could be obtained if the strength of the hydrogen bonding interaction within $[(C_6F_5)_3B(OH_2)]\cdot H_2O$, i.e. K_6, were known.[24] Since experimental data concerned with the strength of the hydrogen bonding interaction within $[(C_6F_5)_3B(OH_2)]\cdot H_2O$ are not available, we have used calculations to provide an estimate of ca.

(18) The pK_a value for $[2,6\text{-}Bu^t_2C_5H_3NH]^+$ in acetonitrile was determined by measurement of the equilibrium with C_5H_5N (see Experimental Section). For comparison, the corresponding values for other pyridine derivatives are as follows: $[C_5H_5NH]^+$ (12.33), $[2,4\text{-}Me_2C_5H_3NH]^+$ (14.05).[a] In this regard, it should be noted that in aqueous and DMSO solutions, 2,6-$Bu^t_2C_5H_3N$ has an anomalously low basicity compared to those of other pyridine derivatives; in the gas phase, however, the basicity of 2,6-$Bu^t_2C_5H_3N$ is normal.[b,c] (a) Chantooni, M. K., Jr.; Kolthoff, I. M. *J. Am. Chem. Soc.* **1968**, *90*, 3005−3009. (b) Benoit, R. L.; Fréchette, M.; Lefebvre, D. *Can. J. Chem.* **1988**, *66*, 1159−1162. (c) Hopkins, H. P., Jr.; Jahagirdar, D. V.; Moulik, P. S.; Aue, D. H.; Webb, H. M.; Davidson, W. R.; Pedley, M. D. *J. Am. Chem. Soc.* **1984**, *106*, 4341−4348.

(19) In this regard, 2,6-di-*tert*-butylpyridine has been shown not to participate readily in hydrogen bond interactions. See: Farcasiu, D.; Lezcano, M.; Vinslava, A. *New J. Chem.* **2000**, *24*, 199−201.

(20) Structurally characterized $[(C_6F_5)_3BOH]^-$ derivatives include the following: $[Cp^*_2Ta(Me)(OH)][(C_6F_5)_3BOH]$,[a] $[Et_3NH][(C_6F_5)_3BOH]$,[b] $[K(dibenzo\text{-}18\text{-}crown\text{-}6)][(C_6F_5)_3BOH]\cdot[(C_6F_5)_3B(OH_2)]\cdot H_2O\cdot MeCHO$,[c] and $\{[Tp^{Bu^t,Me}]Zn(OH_2)\}[HOB(C_6F_5)_3]$.[d] (a) Schaefer, W. P.; Quan, R. W.; Bercaw, J. E. *Acta Crystallogr.* **1993**, *C49*, 878−881. (b) Siedle, A. R.; Newmark, R. A.; Lamanna, W. M.; Huffman, J. C. *Organometallics* **1993**, *12*, 1491−1492. (c) Reference 4b. (d) Reference 6.

(21) The dynamic ^{19}F NMR spectroscopic averaging between $[(C_6F_5)_3B(OH)]^-$ and $[(C_6F_5)_3B(OH_2)]\cdot H_2O$ in the titration experiment was verified by an independent experiment involving addition of $[(C_6F_5)_3B(OH_2)]\cdot H_2O$ to $[Et_3NH][(C_6F_5)_3B(OH)]$.

(22) For structurally characterized examples of the $[(C_6F_5)_3B(\mu\text{-}OH)B(C_6F_5)_3]^-$ anion, see refs 4b and 4c.

(23) Chantooni, M. K., Jr.; Kolthoff, I. M. *J. Am. Chem. Soc.* **1970**, *92*, 2236−2239.

(24) Alternatively, $pK_a = pK_5 - pK_b(H_2O) - pK_6$.

Table 1. Equilibrium Constants for the Various Reactions Studied in Acetonitrile

equation	K	value
$(C_6F_5)_3B(NCMe) + 2H_2O \rightleftarrows [(C_6F_5)_3B(OH_2)]\cdot H_2O + MeCN$	K_1	9(1) M^{-1}
$[(C_6F_5)_3B(OH_2)]\cdot H_2O + 2,6\text{-}Bu^t_2C_5H_3N \rightleftarrows [(C_6F_5)_3BOH]^- + [2,6\text{-}Bu^t_2C_5H_3NH]^+ + H_2O$	K_2	4.2(4) M
$[2,6\text{-}Bu^t_2C_5H_3NH]^+ \rightleftarrows 2,6\text{-}Bu^t_2C_5H_3N + H^+$	K_3	3.7×10^{-12} M
$H_2O + H^+ \rightleftarrows H_3O^+$	K_4[a]	1.6×10^{2} M^{-1}
$[(C_6F_5)_3B(OH_2)]\cdot H_2O \rightleftarrows [(C_6F_5)_3BOH]^- + H_3O^+$	K_5[b]	2.5×10^{-9} M
$[(C_6F_5)_3B(OH_2)]\cdot H_2O \rightleftarrows (C_6F_5)_3B(OH_2) + H_2O$	K_6[c]	4.1×10^{-3} M
$[C_5H_5NH]^+ + 2,6\text{-}Bu^t_2C_5H_3N \rightleftarrows C_5H_5N + [2,6\text{-}Bu^t_2C_5H_3NH]^+$	K_8	0.13
$(C_6F_5)_3B(OH_2) \rightleftarrows [(C_6F_5)_3BOH]^- + H^+$	K_a[d]	3.8×10^{-9} M

[a] Reference 23. [b] $K_5 = K_2K_3K_4$. [c] K_6 at 300 K is estimated using a calculated hydrogen bond energy (neglecting zero point energy differences) and an entropy for dissociation of 15 eu (see text). [d] K_a for $(C_6F_5)_3B(OH_2)$ is K_2K_3/K_6.

Scheme 3

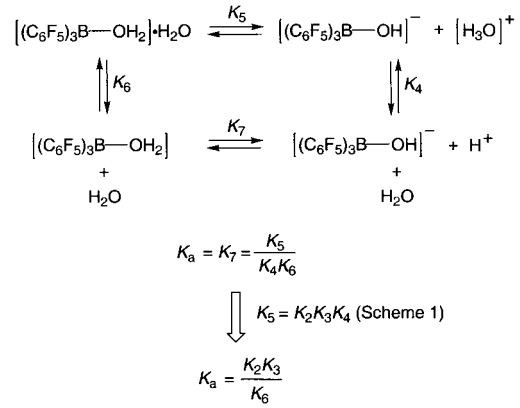

7.8 kcal mol^{-1} for this value in acetonitrile solution (the calculations are described in more detail below). For comparison, the calculated hydrogen bond interaction in $[(C_6F_5)_3B(OH_2)]\cdot H_2O$ is intermediate between the experimentally determined hydrogen bond strengths for $(H_2O)_2$ (5.2 kcal mol^{-1}) and $[(H_2O)_2H]^+$ (31.5 kcal mol^{-1}),[25] and thus represents a reasonable value for such a species. Assuming a value of ca. 15 eu for the entropy involved in breaking the hydrogen bond,[26,27] ΔG_6 at room temperature may be estimated to be ca. 3.3 kcal mol^{-1}, such that $K_6 \approx 4.1 \times 10^{-3}$ M at 300 K. On the basis of this value, K_a for $(C_6F_5)_3B(OH_2)$ may be estimated to be 3.8×10^{-9} M (Scheme 3), from which the pK_a is correspondingly estimated to be 8.4.

Comparison with the pK_a values of other representative acids in acetonitrile (Table 2) indicates that $(C_6F_5)_3B(OH_2)$ must be regarded as a strong acid, with a strength comparable to that of HCl in acetonitrile. Furthermore, since the pK_a values for these acids in acetonitrile are substantially greater, by at least 7.5 pK_a units,[28] than the corresponding acid in water (see, for example, Table 2), it is evident that the hypothetical aqueous pK_a of $(C_6F_5)_3B(OH_2)$ would be expected to be less than ca. 0.9. It should, however, be emphasized that the effective acidity of "hydrated $B(C_6F_5)_3$" will be modulated from this value due to the fact that $(C_6F_5)_3B(OH_2)$ participates in a variety of hydrogen bonding interactions with excess H_2O, and also because the anion $[(C_6F_5)_3BOH]^-$ is capable of forming species such as $[(C_6F_5)_3B(\mu\text{-}OH)B(C_6F_5)_3]^-$ via coordination to $B(C_6F_5)_3$. Nevertheless, it is worth noting that the estimate of 0.9 for the aqueous pK_a value of $(C_6F_5)_3B(OH_2)$ is in close agreement to the value of 1.5 obtained using the pK_a solver of Jaguar (Version 4.0);[29] however, it must be emphasized that the pK_a solver of Jaguar has not been tested with molecules of this type.

Table 2. pK_a Values for a Selection of Acids in MeCN and H_2O

acid	pK_a(MeCN)[a]	pK_a(H_2O)[b]	pK_a(MeCN) − pK_a(H_2O)
H_2SO_4	7.4	ca. −3	10.4
$(C_6F_5)_3B(OH_2)$	8.4		
HCl	8.5	−6.1	14.6
HNO_3	8.9	−1.4	10.3
$[Me_3NH]^+$	17.6	9.8	7.8
$[Bu^n_3NH]^+$	18.1	10.9[c]	7.2
$PhCO_2H$	20.4	4.2	16.2
$MeCO_2H$	22.3	4.8	17.5
PhOH	26.9	10.0	16.9

[a] Data taken from ref 11. For situations in which more than one value is given, it is the average value that is listed. [b] Unless stated otherwise, data were taken from the following: *Lange's Handbook of Chemistry*, 13th ed.; Dean, J. A., Ed.; McGraw-Hill: New York, 1985. [c] Frenna, V.; Vivona, N.; Consiglio, G.; Spinelli, D. *J. Chem. Soc., Perkin Trans. 2* **1985**, 1865−1868.

(ii) Computational Study of Aqua, Alcohol, and Acetonitrile Adducts of $B(C_6F_5)_3$. As indicated above, estimation of the pK_a of $(C_6F_5)_3B(OH_2)$ required knowledge of the strength of the hydrogen bonding interaction within $[(C_6F_5)_3B(OH_2)]\cdot H_2O$. To assess the magnitude of this interaction, we performed ab initio calculations at the B3LYP level on $(C_6F_5)_3B(OH_2)$, $[(C_6F_5)_3B(OH_2)]\cdot H_2O$, and $[(C_6F_5)_3B(OH_2)]\cdot 2H_2O$ using Jaguar (Version 3.5).[29−31] Calculations were also performed at the B3LYP level using a continuum dielectric solvation model to approximate the acetonitrile medium.[32] For further comparisons, we have also performed calculations on the alcohol species, $(C_6F_5)_3B(HOMe)$, $(C_6F_5)_3B(HOBu^t)$, $[(C_6F_5)_3B(HOMe)]\cdot HOMe$, and $[(C_6F_5)_3B(OH_2)]\cdot HOBu^t$. Geometry optimized bond length and angle data are listed in the Supporting Information; comparison with the experimental structures for $(C_6F_5)_3B(OH_2)$ and $[(C_6F_5)_3B(OH_2)]\cdot 2H_2O$ indicates good agreement. The calculated energies associated with the various solvation reac-

(25) For data on hydrogen bond energies, see: (a) Hibbert, F.; Emsley, J. *Adv. Phys. Org. Chem.* **1990**, *26*, 255−379. (b) Emsley, J. *Chem. Soc. Rev.* **1980**, *9*, 91−124.

(26) Entropies of dissociation associated with hydrogen bonding interactions are typically in the range 10−20 eu. See: (a) Arnett, E. M.; Joris, L.; Mitchell, E.; Murty, T. S. S. R.; Gorrie, T. M.; Schleyer, P. v. R. *J. Am. Chem. Soc.* **1970**, *92*, 2365−2377. (b) Kazarian, S. G.; Hamley, P. A.; Poliakoff, M. *J. Chem. Soc., Chem. Commun.* **1992**, 994−997. (c) Jaffé, H. H. *J. Am. Chem. Soc.* **1957**, *79*, 2373−2375.

(27) For a review of entropies for a variety of reactions, see: Minas da Piedade, M. E.; Martinho Simões, J. A. *J. Organomet. Chem.* **1996**, *518*, 167−180.

(28) Note that the minimum difference of ca. 7.5(±1) pK_a units is an estimate which best corresponds to those acids for which the ionic components are large so that the charge is effectively delocalized. For such a situation, the principal change in pK_a in going from acetonitrile to water is due to the differential solvation of H^+. See ref 12a.

(29) Jaguar 3.5 and 4.0, Schrodinger, Inc.: Portland, OR, 1998.

(30) For other recent computational studies on hydrogen bonding interactions involving water, see: Rablen, P. R.; Lockman, J. W.; Jorgensen, W. L. *J. Phys. Chem. A* **1998**, *102*, 3782−3797.

(31) For a recent computational study on the use of $B(C_6F_5)_3$ as a Lewis acid in the generation of metallocene polymerization catalysts, see: Chan, M. S. W.; Vanka, K.; Pye, C. C.; Ziegler, T. *Organometallics* **1999**, *18*, 4624−4636.

(32) Note that the solvation model does not take into account specific hydrogen bonding interactions involving MeCN.

Table 3. Calculated Energetics for the Various Reactions Discussed in the Text

reaction	ΔE (kcal mol^{-1}) B3LYP(gas)	B3LYP(MeCN)	B3LYP(gas) − B3LYP(MeCN)
$B(C_6F_5)_3 + MeCN \rightarrow (C_6F_5)_3B(NCMe)$	−8.32	−10.65	2.32
$B(C_6F_5)_3 + H_2O \rightarrow (C_6F_5)_3B(OH_2)$	−9.38	−11.06	1.68
$(C_6F_5)_3B(OH_2) + H_2O \rightarrow [(C_6F_5)_3B(OH_2)]\cdot H_2O$	−12.90	−7.78	−5.12
$[(C_6F_5)_3B(OH_2)]\cdot H_2O + H_2O \rightarrow [(C_6F_5)_3B(OH_2)]\cdot 2H_2O$	−9.66	−9.33	−0.33
$B(C_6F_5)_3 + MeOH \rightarrow (C_6F_5)_3B(MeOH)$	−5.41	−10.10	4.69
$(C_6F_5)_3B(MeOH) + MeOH \rightarrow [(C_6F_5)_3B(MeOH)]\cdot HOMe$	−14.32	−9.78	−4.54
$B(C_6F_5)_3 + Bu^tOH \rightarrow (C_6F_5)_3B(Bu^tOH)$	−6.44	−7.67	1.23
$(C_6F_5)_3B(OH_2) + Bu^tOH \rightarrow [(C_6F_5)_3B(OH_2)]\cdot HOBu^t$	−16.03	−9.89	−6.15
$(C_6F_5)_3B(OH_2) + MeCN \rightarrow [(C_6F_5)_3B(OH_2)]\cdot NCMe$	−12.25	−6.58	−5.66
$[(C_6F_5)_3B(OH_2)]\cdot H_2O + MeCN \rightarrow [(C_6F_5)_3B(OH_2)]\cdot NCMe\cdot H_2O$	−6.08	−2.11	−3.97
$[C_5H_5NH]^+ + 2,6\text{-}Bu^t{}_2C_5H_3N \rightarrow C_5H_5N + [2,6\text{-}Bu^t{}_2C_5H_3NH]^+$	−14.02	0.90	−14.92

Table 4. Comparison of Selected Bond Lengths and Angles for the Calculated and Experimentally Determined Structures of $(C_6F_5)_3B(NCMe)$

	$(C_6F_5)_3B(NCMe)$ B3LYP[a]	$(C_6F_5)_3B(NCMe)$ calcd (VWN and BP86; STO)[b]	$(C_6F_5)_3B(NCMe)$ calcd (VWN and BP86; GTO)[a]	$(C_6F_5)_3B(NCMe)$ exptl[a]	$(C_6F_5)_3B(NCMe)$ exptl[b]
B−N	1.607	1.576	1.587	1.610	1.616
N−C	1.148	1.151	1.160	1.130	1.124
C−C	1.452	1.444	1.449	1.448	1.452
$B-C_{av}$	1.634	1.631	1.635	1.630	1.629
B−N−C	180	[c]	179.2	177.2	177.1
N−C−C	180	[c]	180.0	178.9	178.9
$N-B-C_{av}$	103.7	104.6	104.0	104.2	104.0
$C-B-C_{av}$	114.5	[c]	114.4	114.2	114.3

[a] This work. [b] Reference 8. [c] Values not reported.

tions are summarized in Table 3, from which it is worth noting that inclusion of solvation effects using a continuum dielectric solvation model results in the hydrogen-bond energies for the above compounds being weaker than the corresponding gas-phase values, whereas $(C_6F_5)_3B-L$ bond energies are stronger than the corresponding gas-phase values. The increased strength of $(C_6F_5)_3B-L$ bonds in acetonitrile is associated with the fact that $B(C_6F_5)_3$ is not stabilized by the solvent medium since it is nonpolar, whereas $(C_6F_5)_3B-L$, being polar, is stabilized.

The $(C_6F_5)_3B-OH_2$ bond energy (neglecting zero point energy differences) is calculated to be 9.4 kcal mol^{-1}, a value which is comparable to that calculated for F_3B-OH_2 (11.5 kcal mol^{-1}).[33−35] Addition of H_2O to $(C_6F_5)_3B-OH_2$ results in the formation of $[(C_6F_5)_3B(OH_2)]\cdot H_2O$ and $[(C_6F_5)_3B(OH_2)]\cdot 2H_2O$, for which the gas-phase hydrogen bond energies are 12.9 and 9.7 kcal mol^{-1}, respectively. Interestingly, while the $(C_6F_5)_3B-OH_2$ bond energy (9.4 kcal mol^{-1}) is comparable to the hydrogen bond energy in $[(C_6F_5)_3B(OH_2)]\cdot H_2O$ (12.9 kcal mol^{-1}), the corresponding energies in the methanol complexes $(C_6F_5)_3B(HOMe)$ (5.4 kcal mol^{-1}) and $[(C_6F_5)_3B(HOMe)]\cdot HOMe$ (14.3 kcal mol^{-1})[36] are more disparate, such that the hydrogen bonding interaction in the latter complex is considerably stronger than the B−O(H)Me bond energy. The lower B−O(H)R bond energies in $(C_6F_5)_3B(HOMe)$ and $(C_6F_5)_3B(HOBu^t)$, as compared to the $B-OH_2$ bond energy in $(C_6F_5)_3B(OH_2)$, are in accord with the isolation of $[(C_6F_5)_3B(OH_2)]\cdot HOBu^t$ (Figure 4) rather than, for example, $[(C_6F_5)_3B(HOBu)]\cdot H_2O$.

We have also performed ab initio calculations on the acetonitrile complex $(C_6F_5)_3B(NCMe)$ since this species is of importance to the present study. Geometry optimized bond length and angle data for $(C_6F_5)_3B(NCMe)$ are listed in Table 4, which also includes the experimental data for comparison. $(C_6F_5)_3B(NCMe)$ has been previously studied by computational methods (VWN and BP86 using STO basis sets),[8] but the results differ somewhat from those reported here, as illustrated in Table 4. In particular, the calculated B−N bond length in the present study (1.607 Å) is noticeably longer than that previously calculated (1.576 Å). We have also carried out a calculation related to that in the literature,[8] using the VWN and BP86 functional but with GTO basis sets, and have obtained a similar B−N bond length (1.587 Å) to the literature value. Significantly, therefore, the calculated B−N bond length obtained using the B3LYP functional corresponds much more closely to the experimentally determined structure of $(C_6F_5)_3B(NCMe)$ than does that obtained using the VWN and BP86 functional.[8] It is also worth noting that the experimental structure of $(C_6F_5)_3B(NCMe)$ has been previously reported,[8] and compares favorably to that described here (Table 4).

In addition to the discrepancy in the calculated B−N bond lengths, there is a corresponding difference in calculated $(C_6F_5)_3B-NCMe$ bond energies. Thus, the $(C_6F_5)_3B-NCMe$ bond energy of 8.3 kcal mol^{-1} [37] reported here is significantly weaker than the value of 15.3 kcal mol^{-1} previously reported;[8] it is, however, comparable to that calculated for $F_3B-NCMe$ (9.1 kcal mol^{-1}).[38]

The thermodynamic cycle summarized in Scheme 4 indicates that, including a continuum dielectric model for solvation by MeCN, the reaction between $(C_6F_5)_3B-NCMe$ and H_2O to give $[(C_6F_5)_3B(OH_2)]\cdot H_2O$ is calculated to be exothermic by −8.2 kcal mol^{-1}. This value compares favorably with the experimentally determined estimate of −8.6 kcal mol^{-1}, which thereby lends support for the accuracy of the calculations.

(33) Sana, M.; Leroy, G.; Wilante, C. *Organometallics* **1992**, *11*, 781−787.

(34) Calculations on H_3B-OH_2 using different levels of theory indicate a rather large range of B−O bond energies (ca. 9−18 kcal mol^{-1}). See ref 33 and the following: Sana, M.; Leroy, G. *Int. J. Quantum Chem.* **1993**, *48*, 89−108.

(35) For other calculations on $(C_6F_5)_3B-L$ adducts, see ref 8.

(36) For further comparison, the hydrogen bond energy in $(MeOH)_2$ (7.6 kcal mol^{-1}) is stronger than that in $(H_2O)_2$ (5.2 kcal mol^{-1}). See ref 25a.

(37) The VWN and BP86 functional using GTO basis sets resulted in a value of 10.0 kcal mol^{-1}.

(38) Jonas, V.; Frenking, G.; Reetz, M. T. *J. Am. Chem. Soc.* **1994**, *116*, 8741−8753.

Scheme 4

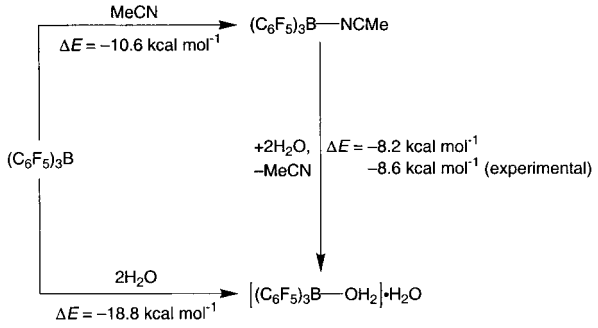

Calculated energy changes (B3LYP including solvation model)

To test further the accuracy of the MeCN dielectric solvent model, calculations were performed on two of the equilibria measured during this study, namely (i) dissociation of H_3O^+ from $[(C_6F_5)_3B(OH_2)]\cdot H_2O$ (K_5) and (ii) the exchange between pyridinium and di-*tert*-butylpyridine (K_8). In both cases, the

$$[C_5H_5NH]^+ + 2,6\text{-}Bu^t{}_2C_5H_3N \underset{}{\overset{K_8}{\rightleftharpoons}} C_5H_5N + [2,6\text{-}Bu^t{}_2C_5H_3NH]^+ \quad (8)$$

calculated and experimental values agree to within 1 pK unit: (i) pK_5(expt) = 8.60 and pK_5(calc) = 7.94,[39] and (ii) pK_8(expt) = 0.89 and pK_8(calc) = 0.66.[40]

(iii) Kinetics of Dissociation of H_2O and MeCN from $(C_6F_5)_3B(OH_2)$ and $(C_6F_5)_3B(NCMe)$. $(C_6F_5)_3B(OH_2)$ and $(C_6F_5)_3B(NCMe)$ are only two of many adducts of the type $(C_6F_5)_3B-L$ formed from the interaction of $B(C_6F_5)_3$ with a Lewis base. Other examples of Lewis bases that are known to coordinate to $B(C_6F_5)_3$ include Ph_3PCH_2,[7] RCN,[8] RNC,[8] R_3P,[3b,8,41] RCHO,[42] R_2CO,[42] $PhCO_2Et$,[42] $PhC(O)NPr^i{}_2$,[42] CN^-,[43] and metal oxo complexes.[44,45] Despite this significant number of $(C_6F_5)_3B-L$ adducts, however, we are only aware of one such study on the kinetics of ligand dissociation for these complexes, namely that for $(C_6F_5)_3B(PH_3)$.[41] Therefore, we considered it appropriate to perform such studies on $(C_6F_5)_3B(OH_2)$ and $(C_6F_5)_3B(NCMe)$, since the equilibrium study described above (eq 1) indicated that the aqua and acetonitrile ligands are labile in this system.

The kinetics of dissociation of acetonitrile from $(C_6F_5)_3B$-(NCMe) in toluene may be conveniently determined by monitoring exchange between coordinated and free acetonitrile (eq 9) using dynamic ^{1}H NMR spectroscopy. Although the coales-

$$(C_6F_5)_3B{-}NCMe + MeCN^* \underset{k_9}{\overset{k_9}{\rightleftharpoons}} (C_6F_5)_3B{-}{}^*NCMe + MeCN \quad (9)$$

cence behavior observed in this system (see Supporting Information) demonstrates that MeCN readily exchanges with $(C_6F_5)_3B(NCMe)$, it does not, per se, indicate the mechanism of the exchange, for which at least two possibilities exist. Thus, the exchange may occur via either (i) a dissociative mechanism, comprising a two-step reaction with initial dissociation of MeCN, or (ii) an associative reaction involving a symmetric intermediate/transition state (Scheme 5). The molecularity of

Scheme 5

Mechanism (i): dissociative

$$(C_6F_5)_3B{-}NCMe \rightleftharpoons (C_6F_5)_3B + MeCN$$

$$MeCN^* + B(C_6F_5)_3 \rightleftharpoons MeCN^*{-}B(C_6F_5)_3$$

Mechanism (ii): associative

$$MeCN^* + (C_6F_5)_3B{-}NCMe \rightleftharpoons [MeCN^*{-}(C_6F_5)_3B{-}NCMe]$$

$$[MeCN^*{-}(C_6F_5)_3B{-}NCMe] \rightleftharpoons MeCN^*{-}B(C_6F_5)_3 + MeCN$$

the reaction has been determined by observing the line broadening[46] as a function of the concentration of both $(C_6F_5)_3B(NCMe)$ and MeCN.[47] Specifically, for a dissociative mechanism (i) the line widths of resonances due to $(C_6F_5)_3B(NCMe)$ are independent of the concentration of both components, whereas (ii) the line widths of resonances due to MeCN are directly proportional to the concentration of $(C_6F_5)_3B(NCMe)$, but inversely proportional to the concentration of MeCN. In contrast, for an associative reaction (i) the line widths of resonances due to $(C_6F_5)_3B(NCMe)$ are independent of the concentration of $(C_6F_5)_3B(NCMe)$, but directly proportional to the concentration of MeCN, whereas (ii) the line widths of resonances due to MeCN are independent of concentration of MeCN, but directly proportional to the concentration of $(C_6F_5)_3B(NCMe)$.

A study of the line broadening as a function of the concentrations of both $(C_6F_5)_3B(NCMe)$ and MeCN clearly indicates that the mechanism is dissociative. Thus, the line widths of resonances due to $(C_6F_5)_3B(NCMe)$ are independent of the concentration of both components, whereas the line widths of resonances due to MeCN are directly proportional to the concentration of $(C_6F_5)_3B(NCMe)$, but inversely proportional to the concentration of MeCN (see Supporting Information).

Analysis of the line widths yields the NMR exchange rate constant k_{NMR} which, for a dissociative reaction, is equal to the dissociation rate constant $k_{diss(MeCN)}$. The temperature dependence of $k_{diss(MeCN)}$ over the range 280−330 K gives rise to the following activation parameters: $\Delta H^‡ = 21.8(5)$ kcal mol^{-1} and $\Delta S^‡ = 23$ (2) eu (Table 5 and Figure 6). Consideration of the reverse reaction indicates that there is a significant barrier for

(39) Assuming a value of 23 eu for ΔS, which is the average experimentally measured gas-phase value for deprotonation of alcohols (22−25.5 eu). See: Bartmess, J. E.; Scott, J. A.; McIver, R. T, Jr. *J. Am. Chem. Soc.* **1979**, *101*, 6046−6056.

(40) Assuming a value of 0 eu for ΔS.

(41) Bradley, D. C.; Hawkes, G. E.; Haycock, P. R.; Sales, K. D.; Zheng, D. H. *Philos. Trans. R. Soc. London A* **1994**, *348*, 315−322.

(42) Parks, D. J.; Piers, W. E.; Parvez, M.; Atencio, R.; Zaworotko, M. J. *Organometallics* **1998**, *17*, 1369−1377.

(43) Lancaster, S. J.; Walker, D. A.; Thornton-Pett, M.; Bochmann, M. *Chem. Commun.* **1999**, 1533−1534.

(44) (a) Barrado, G.; Doerrer, L.; Green, M. L. H.; Leech, M. A. *J. Chem. Soc., Dalton Trans.* **1999**, 1061−1066. (b) Galsworthy, J. R.; Green, J. C.; Green, M. L. H.; Müller, M. *J. Chem. Soc., Dalton Trans.* **1998**, 15−19. (c) Galsworthy, J. R.; Green, M. L. H.; Müller, M.; Prout, K. *J. Chem. Soc., Dalton Trans.* **1997**, 1309−1313. (d) Doerrer, L. H.; Galsworthy, J. R.; Green, M. L. H.; Leech, M. A.; Müller, M. *J. Chem. Soc., Dalton Trans.* **1998**, 3191−3194. (e) Doerrer, L. H.; Galsworthy, J. R.; Green, M. L. H.; Leech, M. A. *J. Chem. Soc., Dalton Trans.* **1998**, 2483−2487. (f) Reference 20b.

(45) Metal−alkyl complexes also form adducts with $B(C_6F_5)_3$. See, for example: Bochmann, M. *J. Chem. Soc., Dalton Trans.* **1996**, 255−270.

(46) In the slow exchange limit, the line width ($w_{1/2}$) is related to the exchange rate constant via the following expression: $w_{1/2} = (1/\pi)[k + (1/T_2)]$. See: Sandström, J. *Dynamic NMR Spectroscopy*; Academic Press: New York, 1982.

(47) For an exchange reaction between AL and L in which the rate expression is rate = $k[AL]^x[L]^y$, the effective first-order rate constant associated with line broadening of resonances attributed to AL is $k[AL]^{x-1}[L]^y$, while that of the resonances attributed to L is $k[AL]^x[L]^{y-1}$. See, for example: Drago, R. S. *Physical Methods for Chemists*; Surfside Scientific Publishers: Gainesville, FL, 1992; pp 295−296.

Table 5. Rate Constants for Dissociation of MeCN from $(C_6F_5)_3B(NCMe)$

T/K	k_9/s^{-1}	T/K	k_9/s^{-1}
280	6.11	316	4.67×10^2
290	2.10×10^1	320	9.67×10^2
300	7.42×10^1	330	2.56×10^3
310	2.81×10^2		

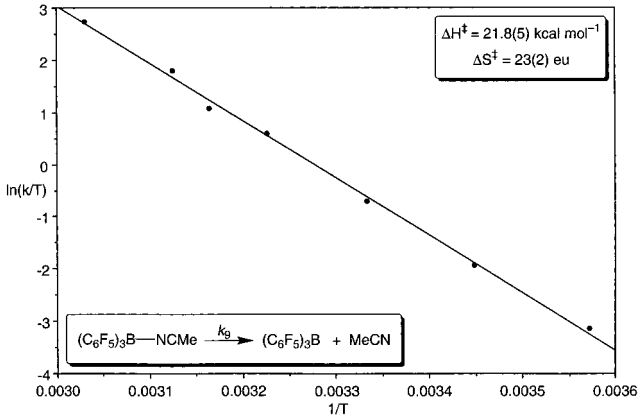

Figure 6. Eyring plot for dissociation of MeCN from $(C_6F_5)_3B(NCMe)$.

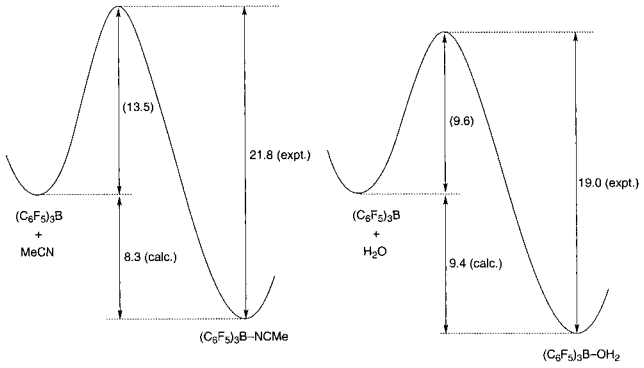

Figure 7. Semiquantitative energy surface for dissociation of MeCN and H_2O from $(C_6F_5)_3B(NCMe)$ and $(C_6F_5)_3B(OH_2)$, respectively (kcal mol^{-1}). The calculated values are gas-phase B3LYP values and the values in parentheses are derived from the other values given.

addition of MeCN to the boron center (Figure 7). Undoubtedly, a large portion of this barrier is due to the geometric reorganization of $B(C_6F_5)_3$ from trigonal planar to the pyramidal geometry present in $(C_6F_5)_3B(NCMe)$, which, in the absence of forming a B−NCMe bond, is calculated to be endothermic by 19.1 kcal mol^{-1}.

In view of the fact that $(C_6F_5)_3B(OH_2)$ forms stable hydrogen-bonded adducts with water, $[(C_6F_5)_3B(OH_2)]\cdot nH_2O$, the kinetics of dissociation cannot be conveniently measured by monitoring exchange between coordinated and free water. Nevertheless, the kinetics of water dissociation in toluene can be studied by observing aqua ligand transfer between $(C_6F_5)_3B(OH_2)$ and $B(C_6F_5)_3$ using variable-temperature ^{19}F NMR spectroscopy (Figure 8). Thus, at 250 K a static spectrum is observed with separate signals corresponding to a mixture of $(C_6F_5)_3B(OH_2)$ and $B(C_6F_5)_3$, whereas the room temperature spectrum is dynamically averaged by the exchange process illustrated in eq 10. The coalescence behavior illustrated in Figure 8 may be

$$(C_6F_5)_3B{-}OH_2 + B^*(C_6F_5)_3 \underset{k_{10}}{\overset{k_{10}}{\rightleftharpoons}} (C_6F_5)_3B + H_2O{-}B^*(C_6F_5)_3 \quad (10)$$

rationalized by two exchange mechanisms, namely (i) a dissociative mechanism, comprising a two-step reaction with initial dissociation of H_2O, or (ii) an associative reaction involving a symmetric intermediate/transition state with a bridging water molecule. As with the MeCN exchange reaction described above, the concentration dependence of the line widths indicates that the mechanism is dissociative. Thus, (i) the line widths of resonances due to $(C_6F_5)_3B(OH_2)$ are independent of the concentration of both components, whereas (ii) the line widths of resonances due to $B(C_6F_5)_3$ are directly proportional to the concentration of $(C_6F_5)_3B(OH_2)$, but inversely proportional to the concentration of $B(C_6F_5)_3$ (see Supporting Information).

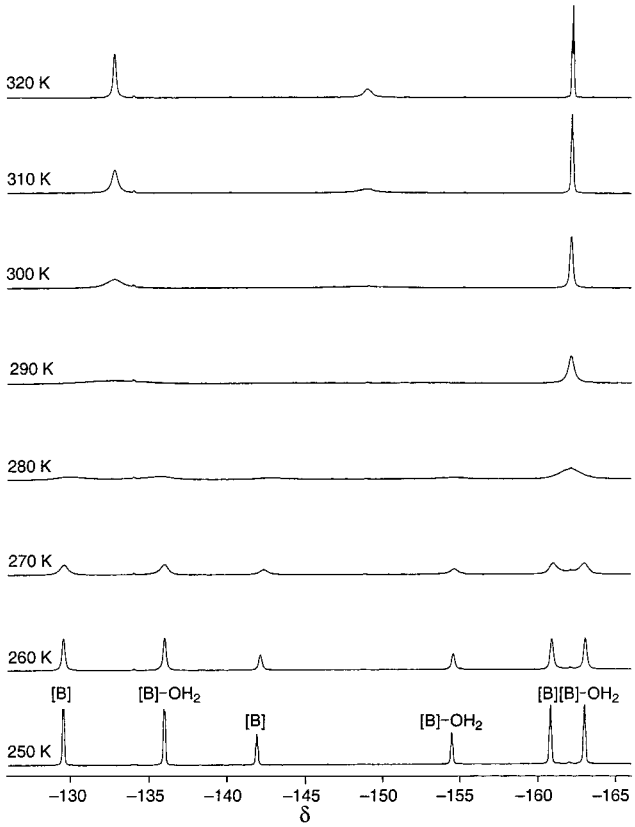

Figure 8. Variable-temperature ^{19}F NMR spectra demonstrating exchange of water between $(C_6F_5)_3B(OH_2)$ and $B(C_6F_5)_3$.

Table 6. Rate Constants for Dissociation of H_2O from $(C_6F_5)_3B(OH_2)$

T/K	k_{10}/s^{-1}	T/K	k_{10}/s^{-1}
260	1.08×10^2	300	1.56×10^4
270	4.68×10^2	310	4.60×10^4
280	1.85×10^3	320	1.50×10^5
290	5.97×10^3		

Since the exchange mechanism is dissociative, the NMR exchange rate constant k_{NMR} is identical with that for dissociation of H_2O ($k_{diss(H_2O)}$). The temperature dependence of $k_{diss(H_2O)}$ over the range 260−320 K gives rise to the following activation parameters: $\Delta H^{\ddagger} = 19.0(3)$ kcal mol^{-1} and $\Delta S^{\ddagger} = 24(1)$ eu (Table 6 and Figure 9). The barrier for dissociation of water is, therefore, less than that for acetonitrile [21.8(5) kcal mol^{-1}] (Figure 7);[48] for example, the rate of dissociation of H_2O is a factor of ca. 200 (at 300 K) greater than that for dissociation of MeCN. These barriers are, however, considerably smaller than

(48) Furthermore, the study also suggests that the barrier for addition of water to $B(C_6F_5)_3$ is less than that for addition of MeCN by ca 3.9 kcal mol^{-1}. The reorganization energy associated with the $B(C_6F_5)_3$ fragment upon addition of water (22.1 kcal mol^{-1}) is, however, calculated to be slightly greater than that for addition of MeCN (19.1 kcal mol^{-1}).

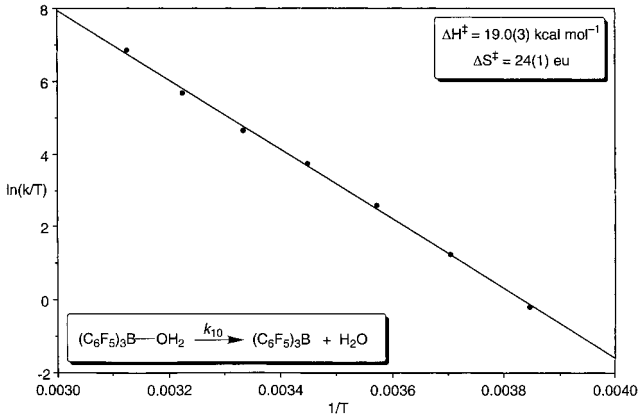

Figure 9. Eyring plot for dissociation of H_2O from $(C_6F_5)_3B(OH_2)$.

that for dissociation of PH_3 from $(C_6F_5)_3B(PH_3)$ [30.1 kcal mol^{-1}].[41]

Experimental Section

General Considerations. All manipulations were performed using a combination of glovebox, high-vacuum, or Schlenk techniques.[49] Solvents were purified and degassed using standard procedures. CD_3CN was purified by passing through a column of $CuSO_4$, followed by sequential vacuum transfer from P_2O_5 (discarding the first 1%) and CaH_2. ^1H and ^{13}C NMR spectra were measured on Bruker Avance 300 DRX and 300wb DRX spectrometers. ^{19}F NMR spectra were measured on a Bruker Avance 300 DRX spectrometer and were referenced relative to $CFCl_3$ ($\delta = 0.00$ ppm) using external $PhCF_3$ ($\delta = -63.72$) as a calibrant.[50] IR spectra were recorded as KBr disks or as solutions on a Perkin-Elmer Spectrum 2000 spectrophotometer. Elemental analyses were performed on a Perkin-Elmer 2400 CHN Elemental Analyzer. $B(C_6F_5)_3$ was a gift from Boulder Scientific; pyridinium triflate and 2,6-di-*tert*-butylpyridine were obtained from Aldrich. All equilibrium and kinetics studies were carried out at 300 K unless stated otherwise.

Synthesis of $(C_6F_5)_3B(OH_2)$. $(C_6F_5)_3B(OH_2)$ was prepared by a method similar to that previously reported.[3b] A solution of $B(C_6F_5)_3$ (1.00 g, 1.95 mmol) in pentane (60 mL) was treated with H_2O (35 μL, 1.94 mmol), thereby resulting in the immediate formation of a white precipitate. The mixture was allowed to stir for 1 h and then filtered. The precipitate was washed with pentane (5 mL) and dried in vacuo giving $(C_6F_5)_3B(OH_2)$ as a white solid (783 mg, 76% yield). Anal. Calcd for $C_{18}H_2OBF_{15}$: C, 40.8; H, 0.4. Found: C, 40.3; H, 0.0. IR data (C_6H_6, cm^{-1}): 3510 (m), 3396 (br) [ν(O−H)], 1648 (s), 1382 (m), 1295 (m), 1112 (s), 793 (w), 776 (w). ^{13}C NMR (C_6D_6): 137.7 [d, $^1J_{C-F} = 272$], 141.3 [d, $^1J_{C-F} = 270$], 148.0 [d, $^1J_{C-F} = 241$] (the *ipso* carbon is unobserved). ^{19}F NMR (C_6D_6): −135.4 [m, *ortho*], −154.0 [br, *para*], −162.9 [m, *meta*].

Synthesis of $[(C_6F_5)_3B(OH_2)]\cdot HOBu^t$. Bu^tOH (25 μL, 0.26 mmol) and H_2O (5 μL, 0.30 mmol) were sequentially added to a suspension of $B(C_6F_5)_3$ (135 mg, 0.264 mmol) in pentane (5 mL), resulting in the immediate formation of a new white precipitate. The mixture was stirred for 1 h at room temperature, allowed to settle overnight, and filtered. The precipitate was dried in vacuo giving $[(C_6F_5)_3B(OH_2)]\cdot HOBu^t$ as a white powder (124 mg, 79%). Anal. Calcd for $C_{22}H_{12}O_2BF_{15}$: C, 43.7; H, 2.0. Found: C, 43.7; H, 1.3. IR data (KBr, cm^{-1}): 3604 (m), 2987 (w), 1651 (s), 1523 (vs), 1472 (vs), 1381 (s), 1286 (m), 1229 (m), 1183 (m), 1103 (s), 970 (vs), 884 (m), 800 (w), 773 (m), 741 (w), 707 (w), 676 (m), 626 (w), 577 (w), 482 (w). ^1H NMR (C_6D_6): 0.52 [s, (CH_3)$_3$COH] (hydroxyl proton not observed). ^{19}F NMR (C_6D_6): −135.8 [m, *ortho*], −156.3 [t, $^3J_{F-F} = 20$, *meta*], −163.9 [m, *para*].

Synthesis of $[(C_6F_5)_3B(HOMe)]\cdot HOMe$. $[(C_6F_5)_3B(HOMe)]\cdot HOMe$ was prepared by a slight modification of a previously reported method.[3a] MeOH (40 μL, 0.988 mmol) was added to a suspension of $B(C_6F_5)_3$ (250 mg, 0.488 mmol) in pentane (5 mL), thereby resulting in the immediate formation of a new white precipitate. The mixture was stirred for 1 h at room temperature and filtered. The precipitate was dried in vacuo giving $[(C_6F_5)_3B(HOMe)]\cdot HOMe$ as a white solid (184 mg, 69%). Anal. Calcd for $C_{20}H_8BF_{15}O_2$: C, 41.7; H, 1.4. Found: C, 42.2; H, 0.2. IR data (KBr, cm^{-1}): 3633 (m), 3523 (m), 1651 (m), 1523 (s), 1470 (s), 1380 (m), 1287 (m), 1106 (s), 980 (s), 867 (m), 800 (m), 774 (m), 752 (w), 714 (w), 677 (m), 619 (w), 576 (w), 456 (w). ^1H NMR (C_6D_6): 2.50 [s, 2CH_3OH], hydroxyl not observed. ^{13}C NMR (C_6D_6): 52.3 [2 CH_3OH], 137.5 [d, $^1J_{C-F} = 242$], 140.8 [d, $^1J_{C-F} = 252$], 148.2 [d, $^1J_{C-F} = 244$], 115.8 [broad, *ipso*] (C_6F_5). ^{19}F (C_6D_6): −135.4 [m, $^3J_{F-F} = 21$, *ortho*], −155.5 [m, $^3J_{F-F} = 21$, *para*], −163.4 [m, *meta*].

Synthesis of $(C_6F_5)_3B(NCMe)$. $(C_6F_5)_3B(NCMe)$ was prepared by a method similar to that previously reported.[8] A suspension of $B(C_6F_5)_3$ (145 mg, 283 mmol) in pentane (5 mL) was treated with CH_3CN (50 μL, 957 mmol), resulting in the formation of a new white precipitate. The mixture was allowed to stir for 1 h and filtered. The precipitate was dried in vacuo, giving $(C_6F_5)_3B(NCMe)$ as a white solid (122 mg, 78% yield). IR data (KBr, cm^{-1}): 2939 (vw), 2367 (m), 1651 (m), 1523 (s), 1471 (vs), 1386 (m), 1288 (m), 1109 (s), 972 (s), 794 (w), 775 (m), 741 (w), 683 (m), 621 (w). ^1H NMR (C_6D_6): 0.25 [s, CH_3CN]. ^{19}F NMR (C_6D_6): −135.3 [m, *ortho*], −155.8 [t, $^3J_{F-F} = 21$, *meta*], −163.7 [m, *para*].

Determination of the Equilibrium Constant (K_1) for the Reaction between $(C_6F_5)_3B(NCMe)$ and H_2O Giving $(C_6F_5)_3B(OH_2)\cdot(H_2O)$ in CD_3CN. A solution of $(C_6F_5)_3B(OH_2)$ (8.8 mg, 0.017 mmol) in CD_3CN (0.50 mL) was treated with aliquots of a solution of H_2O in CD_3CN (0.66 M). After each addition, the relative amounts of $(C_6F_5)_3B(NCMe)$ and $[(C_6F_5)_3B(OH_2)]\cdot H_2O$ were determined by measurement of the ^{19}F NMR spectrum at 300 K. Water concentrations were converted to activities using the activity coefficient of water in acetonitrile.[51,52] The stoichiometry of the aqua species formed in acetonitrile solution, $(C_6F_5)_3B(OH_2)_n$, was determined by comparing a fit of the data using values of n from 1 to 3 (see Figure 2). The equilibrium constant (K_1) at room temperature was determined from a plot of the ratio $[(C_6F_5)_3B(OH_2)_2]/[(C_6F_5)_3B(NCMe)]$ vs $\{\gamma[H_2O]\}^2$, in which the slope is equal to $K_1/[CD_3CN]$, where $[CD_3CN] = 19.15$ M. The temperature dependence of the equilibrium was studied using a sample with a large excess of H_2O (concentration = 0.25 M; activity = 2.54 M) compared to total boron reagent (0.028 M), such that the activity of water remains effectively constant as the equilibrium reestablishes.

Determination of the Equilibrium Constant (K_2) for Deprotonation of $[(C_6F_5)_3B(OH_2)]\cdot H_2O$ by 2,6-Di-*tert*-butylpyridine. An equilibrium mixture of $[(C_6F_5)_3B(OH_2)]\cdot H_2O$ and $(C_6F_5)_3B(NCMe)$ in acetonitrile was prepared by dissolving $(C_6F_5)_3B(OH_2)$ (10.2 mg, 0.019 mmol) in CD_3CN (0.50 mL). This solution was treated with 11 aliquots of a solution of 2,6-di-*tert*-butylpyridine in CD_3CN (0.326 M) and the relative amounts of the species present at equilibrium were determined by NMR spectroscopy at 300 K. The concentration of each species was calculated according to the following procedure and then combined to give K_2. The concentrations of $[2,6\text{-}Bu^t_2C_5H_3N]^+$ and $[2,6\text{-}Bu^t_2C_5H_3NH]^+$ were determined by ^1H NMR spectroscopy and pyridine mass balance. The concentration of $[(C_6F_5)_3BOH]^-$ was determined by charge balance with $[2,6\text{-}Bu^t_2C_5H_3NH]^+$. Due to rapid exchange between $(C_6F_5)_3B(H_2O)\cdot(H_2O)$ and $[(C_6F_5)_3BOH]^-$, ^{19}F NMR spectroscopy provided only the ratio of $(C_6F_5)_3B(NCMe)$ to the total of the aforementioned aqua/hydroxide species but, together with consideration of boron mass balance, the individual concentrations of $(C_6F_5)_3B(H_2O)\cdot(H_2O)$ and $(C_6F_5)_3B(NCMe)$ may be calculated since the concentration of $[(C_6F_5)_3BOH]^-$ is known from above. The activity of the water, $\{\gamma$-

(49) (a) McNally, J. P.; Leong, V. S.; Cooper, N. J. In *Experimental Organometallic Chemistry*; Wayda, A. L., Darensbourg, M. Y., Eds.; American Chemical Society: Washington, DC, 1987; Chapter 2, pp 6−23. (b) Burger, B. J.; Bercaw, J. E. In *Experimental Organometallic Chemistry*; Wayda, A. L., Darensbourg, M. Y., Eds.; American Chemical Society: Washington, DC, 1987; Chapter 4, pp 79−98.

(50) Evans, B. J.; Doi, J. T.; Musker, W. K. *J. Org. Chem.* **1990**, *55*, 2337−2344.

(51) (a) Bell, G.; Janssen, A. E. M.; Halling, P. J. *Enzyme Microb. Technol.* **1997**, *20*, 471−477. (b) There were several typographic errors in the formulae given. (Halling, P. J., personal communication and http://homepages.strath.ac.uk/~cdbs05/watmeth.htm).

(52) Eggers, D. F., Jr.; Gregory, N. W.; Halsey, G. D., Jr.; Rabinovitch, B. S. *Physical Chemistry*; John Wiley and Sons: New York, 1964; Chapter 10.

Table 7. Crystal, Intensity Collection, and Refinement Data

	$(C_6F_5)_3B(NCMe)$	$(C_6F_5)_3B(OH_2)$	$[(C_6F_5)_3B(OH_2)]\cdot HOBu^t$	$[(C_6F_5)_3B(HOMe)]\cdot HOMe$
lattice	monoclinic	monoclinic	monoclinic	triclinic
formula	$C_{20}H_3BF_{15}N$	$C_{18}H_2BF_{15}O$	$C_{22}H_{12}BF_{15}O_2$	$C_{20}H_8BF_{15}O_2$
formula weight	553.04	530.01	604.13	576.07
space group	$P2_1/n$ (No. 14)	$P2_1/n$ (No. 14)	$C2/c$ (No. 15)	$P\bar{1}$ (No. 2)
a/Å	10.9478(7)	10.8703(6)	21.516(3)	9.0464(7)
b/Å	9.2910(6)	11.5164(7)	12.1170(12)	10.2064(8)
c/Å	19.4038(12)	14.6410(9)	19.835(3)	12.6339(10)
α/deg	90	90	90	75.170(1)
β/deg	90.369(1)	98.065(1)	115.925(4)	71.776(1)
γ/deg	90	90	90	82.275(2)
V/Å^3	1973.6(2)	1814.7(2)	4651(1)	1069.2(2)
Z	4	4	8	2
temp (K)	213	203	218	223
radiation (λ, Å)	0.71073	0.71073	0.71073	0.71073
ρ (calcd), g cm^{-3}	1.861	1.940	1.726	1.789
μ (Mo Kα), mm^{-1}	0.21	0.23	0.19	0.20
θ max, deg	28.3	28.3	28.7	28.4
no. of data	4591	4211	5384	4704
no. of parameters	336	325	377	354
R_1	0.0433	0.0429	0.0587	0.0405
wR_2	0.0955	0.0922	0.1138	0.1143
GOF	1.013	1.012	1.018	1.052

$[H_2O]\}$, is determined from the concentrations of $(C_6F_5)_3B(H_2O)\cdot(H_2O)$ and $(C_6F_5)_3B(NCMe)$ using the value of K_1 for equilibrium 1. A value of K_2 was calculated after addition of each aliquot. The experiment was repeated and the average value of K_2 obtained by this procedure is 4.2(4).

Determination of the pK_a of 2,6-Di-*tert*-butylpyridine. A solution of $[C_5H_5NH][CF_3SO_3]$ (5.9 mg, 0.026 mmol) in CD_3CN (500 μL) was treated with 25 μL aliquots of a solution of 2,6-$Bu^t_2C_5H_3N$ in CD_3CN (0.48 M) and the ^{1}H NMR spectrum was recorded after each addition. Since fast exchange is observed between the protonated and deprotonated species for both reagents, the averaged chemical shifts were used to determine the concentration of the various species present in solution. To do this, an authentic sample of $[2,6\text{-}Bu^t_2C_5H_3NH][CF_3SO_3]$ was prepared by reaction of 2,6-$Bu^t_2C_5H_3N$ with CF_3SO_3H. It was also necessary to take into account the self-association equilibrium involving C_5H_5N and $[C_5H_5NH]^+$ [53] prior to determining the equilibrium constant for the reaction between $[C_5H_5NH]^+$ and 2,6-$Bu^t_2C_5H_3N$ (eq 8; K = 0.13, pK = 0.89).[54] Finally, the pK_a of $[2,6\text{-}Bu^t_2C_5H_3NH]^+$ was determined to be 11.4 by consideration of the above pK value and the literature pK_a value of $[C_5H_5NH]^+$ (12.3) in CH_3CN.[55]

Determination of the Kinetics for Dissociation of MeCN from $(C_6F_5)_3B(NCMe)$. The ^{1}H NMR spectrum of a solution of $(C_6F_5)_3B(NCMe)$ (9.5 mg, 0.017 mmol) and CH_3CN (0.9 mg, 0.02 mmol) in toluene-d_8 (0.6 mL) was recorded over the temperature range 280−330 K. The exchange rate was determined at each temperature using the spectral simulation program gNMR,[56] as summarized in Table 5 (the ^{1}H NMR spectrum recorded at 255 K was used to determine the line widths of the peaks in the absence of exchange). Evidence for a dissociative mechanism was obtained by observing the dependence of the NMR spectroscopic rate of exchange on the concentrations of $(C_6F_5)_3B(NCMe)$ and MeCN (see Results and Discussion). Thus, (i) the line widths of resonances due to $(C_6F_5)_3B(NCMe)$ are independent of the concentration of both components, whereas (ii) the line widths of resonances due to MeCN are directly proportional to the concentration of $(C_6F_5)_3B(NCMe)$, but inversely proportional to the concentration of MeCN.

Determination of the Kinetics for Dissociation of H_2O from $(C_6F_5)_3B(OH_2)$. The ^{19}F NMR spectrum of a mixture of $(C_6F_5)_3B(OH_2)$ (5.0 mg, 0.009 mmol) and $B(C_6F_5)_3$ (5.0 mg, 0.010 mmol) in toluene-d_8 was recorded over the range 250−320 K, at 10 K intervals. The exchange rate at each temperature was obtained by spectral simulation using gNMR,[56] as summarized in Table 6. Evidence for a dissociative mechanism was obtained by observing the dependence of the NMR spectroscopic rate of exchange on the concentrations of $(C_6F_5)_3B(OH_2)$ and $B(C_6F_5)_3$ (see Results and Discussion). Thus, (i) the line widths of resonances due to $(C_6F_5)_3B(OH_2)$ are independent of the concentration of both components, whereas (ii) the line widths of resonances due to $B(C_6F_5)_3$ are directly proportional to the concentration of $(C_6F_5)_3B(OH_2)$, but inversely proportional to the concentration of $B(C_6F_5)_3$.

Computational Details. All calculations were performed using the Jaguar program.[29] Initial geometries were obtained from crystal structures for $(C_6F_5)_3B(OH_2)$, $[(C_6F_5)_3B(HOMe)]\cdot HOMe$, $[(C_6F_5)_3B(OH_2)]\cdot HOBu^t$, and $(C_6F_5)_3B(NCMe)$. The other complexes were built from modification of the coordinates of these crystal structures. DFT geometry optimizations were performed at the B3LYP level using the LACVP** basis set. Single point energies were calculated for the optimized structures at the B3LYP level using the triple ζ basis set CC-PVTZ (-f) for all elements except boron, for which the 6-31G** basis set was used. LDA (local density approximation) calculations were carried out to determine the optimal geometry and B−N bond strength of $(C_6F_5)_3B(NCMe)$ using the Slater local exchange functional and VWN (Vosko−Nusair−Wilk) local correlation functional with Becke 1988 and Perdew 1986 correctional functionals. The basis sets used for the calculations were identical to those used for the B3LYP calculations. MeCN solvation energies were calculated at the B3LYP level with the LACVP** basis set using the Jaguar Poisson−Boltzmann solver. The dielectric was set to 36 and the probe radius was set to 2.18 Å.

X-ray Structure Determinations. Crystal data, data collection, and refinement parameters are summarized in Table 7. X-ray diffraction data were collected on a Bruker P4 diffractometer equipped with a SMART CCD detector. The structures were solved using direct methods and standard difference map techniques, and were refined by full-matrix least-squares procedures using SHELXTL.[57] Hydrogen atoms on carbon were included in calculated positions.

Conclusions

In summary, solutions of $B(C_6F_5)_3$ in acetonitrile in the presence of water exist as an equilibrium mixture of $(C_6F_5)_3B(NCMe)$ and $[(C_6F_5)_3B(OH_2)]\cdot H_2O$. The aqua species $[(C_6F_5)_3B(OH_2)]\cdot H_2O$ is deprotonated upon treatment with 2,6-$Bu^t_2C_5H_3N$, thereby generating $[2,6\text{-}Bu^t_2C_5H_3NH]^+$ and $[(C_6F_5)_3B(OH)]^-$.

(53) The equilibrium constant for $C_5H_5N + [C_5H_5NH]^+ \rightleftarrows [(C_5H_5N)_2H]^+$ is 0.7. See ref 18a.

(54) Self-association giving $[(2,6\text{-}Bu^t_2C_5H_3N)_2H]^+$ is assumed to be negligible due to excessive steric interactions.

(55) Reference 11, p 26.

(56) gNMR (Version 4.1), Cherwell Scientific Ltd.: Oxford.

(57) Sheldrick, G. M. SHELXTL, An Integrated System for Solving, Refining and Displaying Crystal Structures from Diffraction Data; University of Göttingen: Göttingen, Federal Republic of Germany, 1981.

NMR spectroscopic analysis of the deprotonation reaction allows a p*K* value of 8.6 to be determined for the equilibrium $[(C_6F_5)_3B(OH_2)]\cdot H_2O \rightleftarrows [(C_6F_5)_3B(OH)]^- + [H_3O]^+$ in acetonitrile. On the basis that a computational study indicates the strength of the hydrogen bond interaction in $[(C_6F_5)_3B(OH_2)]\cdot H_2O$ to be 7.8 kcal mol^{-1}, the pK_a for $(C_6F_5)_3B(OH_2)$, itself, is estimated to be 8.4 in acetonitrile. Such a value indicates that $(C_6F_5)_3B(OH_2)$ must be regarded as a strong acid, with a strength comparable to that of HCl in acetonitrile. Dynamic NMR spectroscopic studies indicate that the aqua and acetonitrile ligands in $(C_6F_5)_3B(OH_2)$ and $(C_6F_5)_3B(NCMe)$ are labile, with dissociation of H_2O being substantially more facile than that of MeCN. Thus, $\Delta H^{\ddagger}$ for dissociation of H_2O is 19.0(3) kcal mol^{-1}, while that for MeCN is 21.8(5) kcal mol^{-1}, a difference that corresponds to a factor of ca. 200 in rate constant at 300 K.

Acknowledgment. We thank the National Institutes of Health (Grant GM46502 to G.P. and GM40526 to R.A.F.) for support of this research. Barry Dunietz and Dr. Mike Beachy are thanked for helpful discussions.

Supporting Information Available: Crystallographic information, tables of calculated bond lengths, and spectroscopic figures (PDF). This material is available free of charge via the Internet at http://pubs.acs.org.

JA001915G